Clinical Neurophysiology 181 (2026) 2111405

Contents lists available at ScienceDirect

Clinical Neurophysiology

journal homepage: www.elsevier.com/locate/clinph

Cerebellar transcranial direct current stimulation in spinocerebellar ataxia type 3: An electric field modelling study

Roderick P.P.W.M. Maas [a,*], ESMI MR Study Group [1], Jennifer Faber [b,c,d], Bart P.C. van de Warrenburg [a], Dennis J.L.G. Schutter [e]

[a] Department of Neurology, Donders Institute for Brain, Cognition, and Behaviour, Radboud University Medical Center, Nijmegen, the Netherlands
[b] German Center for Neurodegenerative Diseases (DZNE), Bonn, Germany
[c] Center of Neurology, Department of Parkinson's Disease, Sleep and Movement Disorders, University Hospital Bonn, Bonn, Germany
[d] Department of Neuroradiology, University Hospital Bonn, Bonn, Germany
[e] Experimental Psychology, Helmholtz Institute, Utrecht University, Utrecht, the Netherlands

ARTICLE INFO

Keywords:
Ataxia
Cerebellar tDCS
Electric fields
Interindividual variability
Modelling study
Simulation

ABSTRACT

Objectives: To compare cerebellar transcranial direct current stimulation (tDCS)-induced electric field strengths between individuals with spinocerebellar ataxia type 3 (SCA3) and healthy controls and to identify factors that underlie the variability in field strength.
Methods: MRI scans from 68 SCA3 mutation carriers spanning the disease spectrum and 37 healthy adults were used to reconstruct tetrahedral volume meshes of the head. Electric field simulations of midline cerebellar tDCS were performed with the buccinator muscle, frontopolar region, and lower neck as reference electrode positions. Eight regions of interest were defined throughout the cerebellum.
Results: Simulated electric field strengths induced by cerebellar tDCS were generally lower in SCA3 mutation carriers than in healthy controls, particularly in the anterior lobe and with cephalic reference electrodes. The frontopolar montage induced the highest field strengths, while the lower neck montage caused the lowest field strengths. Skin-cerebellum distance, Scale for the Assessment and Rating of Ataxia (SARA) score, and "occipital angle" were independently associated with electric field strength.
Conclusion: Skin-cerebellum distance, posterior fossa morphometry, ataxia severity, and electrode montage predict cerebellar tDCS-induced electric field strength in SCA3 mutation carriers. These results may guide the development of personalized neuromodulation protocols and inform the design of future cerebellar tDCS trials in degenerative ataxias.
Significance: This study identified clinical and anatomical factors that affect cerebellar tDCS-induced field strength in individuals with the most common type of dominantly inherited ataxia worldwide.

1. Introduction

Degenerative ataxias comprise a diverse group of inherited and acquired conditions that share a progressive cerebellar syndrome as their central clinical theme. Because of the established functional diversity of the cerebellar cortex and its dense reciprocal connections with essentially all supratentorial regions, cerebellar neuronal loss usually manifests with various combinations of motor and non-motor symptoms. In particular, damage to the anterior lobe, medial parts of lobule VI, and lobule VIII – collectively referred to as the sensorimotor cerebellum – is associated with gait ataxia, appendicular dysmetria, and dysarthria (Schmahmann, 2019, Stoodley and Schmahmann, 2010). Lesions of lobule VI, Crus I, and Crus II – the cognitive cerebellum – are linked to impairments in executive functions, visuospatial cognition, and linguistic processing. Finally, injuries to the posterior vermis and fastigial nucleus – the limbic cerebellum – have been shown to induce deficits in emotional processing, affect regulation, and eye movements (Schmahmann, 2019, Stoodley et al., 2016, Stoodley and Schmahmann,

* Corresponding author at: Department of Neurology, Donders Institute for Brain, Cognition, and Behaviour, Radboud University Medical Center, Geert Grooteplein Zuid 10, 6525 GA Nijmegen, the Netherlands.
E-mail address: roderick.maas@radboudumc.nl (R.P.P.W.M. Maas).
[1] See the Appendix.

https://doi.org/10.1016/j.clinph.2025.2111405
Accepted 8 October 2025
Available online 26 October 2025

2010).

Novel therapeutic strategies that mitigate motor, cognitive, and affective impairments and enhance quality of life are urgently required in patients with degenerative ataxias. Recent years have witnessed increasing interest in cerebellar non-invasive stimulation techniques as a potential new treatment avenue, aimed at augmenting local cerebellar neuroplasticity and strengthening cerebellocerebral connectivity (Benussi et al., 2023, Maas et al., 2020, Miterko et al., 2019). Computational modelling studies in healthy individuals have established the biophysical feasibility of modulating cerebellar structures using transcranial direct current stimulation (tDCS) over the back of the head (Parazzini et al., 2014, Rampersad et al., 2014). Repeated sessions of cerebellar midline tDCS have subsequently been shown to improve ataxia severity in etiologically heterogeneous groups of patients, accompanied by an increase in cerebellar-motor cortex connectivity (Benussi et al., 2018, Benussi et al., 2017). Inspired by these results, we performed a randomized, double-blind, sham-controlled trial in individuals with spinocerebellar ataxia type 3 (SCA3) – the most common type of dominantly inherited ataxia worldwide – using a similar stimulation protocol (Maas et al., 2022b). Although our study did not demonstrate short-term or long-term treatment effects of tDCS on the group level, clinically relevant improvements in a subset of patients were observed that lasted for several months. Interestingly, more recent tDCS trials in a mixed sample of both degenerative ataxias and cerebellar strokes (Reumers et al., 2025), as well as in Friedreich ataxia (Naeije et al., 2023), confirmed this finding of interindividual variability in treatment response, albeit with overall positive effects on ataxia severity. If proven effective, identifying predictors of treatment success would be highly relevant for clinicians in the ataxia field and may eventually lead to individually tailored tDCS protocols.

Between-subject differences in electric field strength at the target site have been proposed as a contributing factor to the efficacy of tDCS given their associations with changes in functional network connectivity, gamma-aminobutyric acid (GABA) concentrations, and motor-evoked potentials (Antonenko et al., 2019, Laakso et al., 2019, Mosayebi-Samani et al., 2021, Nandi et al., 2022). Approximately 60–70% of the variance in cerebellar tDCS-induced electric field strength and distribution in healthy individuals is explained by skin-cerebellum distance and morphometric posterior fossa features (Gomez-Tames et al., 2019, Klaus and Schutter, 2021, Maas et al., 2023). In addition to anatomical factors, selection of the position of the reference electrode has recently been reported to affect electric field characteristics when applying cerebellar midline tDCS. Specifically, the (cephalic) frontopolar and buccinator montages yielded significantly higher electric field strengths throughout the cerebellum – at the expense of focality – as compared with the (extracephalic) lower neck montage (Maas et al., 2023).

Prior computational modelling studies have focused on healthy controls. An important outstanding question remains to what extent tDCS over the lower occiput is able to target the cerebellum in cerebellar patients at different disease stages, and consequently, which individuals may potentially benefit most from this intervention (Manto et al., 2021). Neuroimaging-based simulation studies of cerebellar tDCS-induced electric fields could provide valuable insights and may guide the development of personalized treatment protocols, but are currently lacking in patients with cerebellar disorders. In this modelling study, we used a large MRI data set from an international cohort of SCA3 mutation carriers and matched healthy controls to evaluate between-group differences in strength and distribution of cerebellar tDCS-induced electric fields within the cerebellum. Furthermore, we comprehensively examined the influence of ataxia severity, individual anatomical characteristics, and electrode montage on electric field strength in SCA3.

2. Methods

2.1. Study design and participants

Eligible participants were SCA3 mutation carriers covering almost the entire disease course (i.e., from pre-ataxic stage to wheelchair-dependency) and healthy controls who had undergone structural brain MR imaging in the prospective, longitudinal European Spinocerebellar ataxia type 3 / Machado-Joseph Disease Initiative (ESMI) cohort study. Clinical data in ESMI were collected at eleven European and two US ataxia referral centers. Sites acquiring MRI scans were Bonn, Nijmegen, Minneapolis, Essen, London, Heidelberg, Baltimore, and Aachen.

Apart from a genetically confirmed SCA3 status and an age $\geq$ 18 years, there were no other specific inclusion or exclusion criteria for mutation carriers. Healthy controls did not have a history of neurological or psychiatric disorders.

The study protocol was approved by the medical ethics committees of contributing centers. Written informed consent was obtained from each participant.

2.2. MRI acquisition

MRI data were acquired using 3 T Siemens scanners with body coil transmission and 32-channel receive phased-array head coils. T1-MPRAGE (repetition time = 2500 ms, echo time = 4.37 ms, inversion time = 1100 ms) and T2-FLAIR sequences (repetition time = 5000 ms, echo time = 397 ms, inversion time = 1800 ms) were recorded in sagittal direction and contained 192 slices. All scans share a 1-mm isotropic resolution and 256 × 256 matrix size.

2.3. Electric field simulations

High-resolution MRI scans were transformed into individualized tetrahedral volume meshes using SimNIBS' *headreco* pipeline (version 3.2.6) (Saturnino et al., 2018). Every head mesh was inspected visually to ensure segmentation accuracy. Starting from four fiducial points (i.e., the nasion, inion, left pre-auricular point, and right pre-auricular point), the software calculates EEG electrode positions according to the international 10–10 system (Jurcak et al., 2007). In keeping with previous randomized controlled trials (Benussi et al., 2018, Benussi et al., 2017, Maas et al., 2022a, Maas et al., 2022b, Reumers et al., 2025), a 4-mm thick rectangular target electrode (7 × 5 cm) was centered in the midline 2 cm below the inion of each head model. Similarly sized reference electrodes were positioned over the right cheek, the middle of the forehead over Fpz, and the lower neck to simulate the buccinator montage, frontopolar montage, and right lower neck montage (as an approximation of the deltoid montage), respectively (Maas et al., 2023).

Following clinical trial practice (Benussi et al., 2018, Benussi et al., 2017, Maas et al., 2022a, Maas et al., 2022b, Reumers et al., 2025), a current intensity of 2 mA was used in all simulations. Standard conductivity values were applied: σ_{scalp} = 0.465 S/m, σ_{skull} = 0.01 S/m, $\sigma_{cerebrospinal\ fluid}$ = 1.654 S/m, $\sigma_{grey\ matter}$ = 0.276 S/m, $\sigma_{white\ matter}$ = 0.126 S/m, and $\sigma_{eye\ balls}$ = 0.50 S/m (Rezaee and Dutta, 2019, Wagner et al., 2004, Windhoff et al., 2013). The field focality of each montage was determined as the volume of grey matter with a field strength equal to or higher than 50% of the 99.9th percentile (Saturnino et al., 2018).

2.4. Regions of interest

Average field strengths were estimated in eight functionally diverse areas of the cerebellar cortex, covering the vermis and hemispheres of the anterior and posterior lobe (Maas et al., 2023). Regions of interest (ROIs) had a radius of 5 mm and were situated in the vermis of lobule V (ROI1; MNI coordinates: x = 0, y = −66, z = −9; involved in postural control), right lobule V (ROI2; MNI coordinates: x = 15, y = −55, z = −16; involved in right hand movements and a finger sequence task), left

lobule V (ROI3; MNI coordinates: x = −18, y = −53, z = −19; involved in left hand movements and a finger sequence task), right Crus II (ROI4; MNI coordinates: x = 24, y = −83, z = −40; involved amongst others in verb generation, word reading, and theory of mind), left Crus II (ROI5; MNI coordinates: x = −23, y = −82, z = −39; involved amongst others in theory of mind and interval timing), the vermis of lobule VIIIA (ROI6; MNI coordinates: x = 0, y = −70, z = −40; involved amongst others in emotional processing, a finger sequencing task, and hand movements), right lobule VIIIA (ROI7; MNI coordinates: x = 21, y = −61, z = −52; involved amongst others in right hand movements and a finger sequence task), and left lobule VIIIA (ROI8; MNI coordinates: x = −21, y = −59, z = −57; involved amongst others in left hand movements and a finger sequence task) (King et al., 2019, Maas et al., 2023). The mni2subject_coords function in SimNIBS was used to transform MNI coordinates to subject space.

2.5. Cerebellar volumetry

The cerebellum was subsegmented into 25 cortical and 2 white matter labels using CerebNet (Faber et al., 2022). Parcellations were inspected visually to ensure segmentation accuracy. Total cerebellar grey matter and total cerebellar white matter volume were selected as the volumes of interest in this study and calculated as the sum of individual cortical and white matter labels, respectively. Brainstem volume and estimated total intracranial volume (eTIV) were obtained with FreeSurfer software.

2.6. Individual anatomical characteristics

Skin-cerebellum distance was determined on each participant's T1-MPRAGE scan, along with four morphometric parameters of the posterior fossa (Maas et al., 2023). The former was defined as the shortest (perpendicular) distance between the skin approximately 2 cm below the inion (i.e., the position of the target electrode's center) and the outer surface of the vermis on a midsagittal slice. In addition to a midline distance, similar measurements were conducted for both hemispheres at points midway between the vermis and the most lateral parts of the cerebellum. The following angles involving posterior fossa structures were measured on a midsagittal MRI slice: (i) tentorial angle (i.e., between a line through the tentorium and a line connecting the nasion and tuberculum sellae), (ii) cerebellar angle (i.e., between a line through the tentorium and a line from the opisthion to the most "curved" position of the posterior fossa cerebrospinal fluid (CSF) space directly behind the cerebellum), (iii) pons angle (i.e., between a line through the dorsal surface of the pons and a line through the tentorium), and (iv) occipital angle (i.e., between a line connecting the nasion and tuberculum sellae and a line from the opisthion through the most curved position of the posterior fossa CSF space directly behind the cerebellum) (Maas et al., 2023).

2.7. Ataxia severity

The Scale for the Assessment and Rating of Ataxia (SARA) was used to quantify the overall severity of ataxia, with a range from 0 (no ataxia) to 40 (most severe ataxia) (Schmitz-Hubsch et al., 2006). Standardized assessments of gait, stance, sitting, speech, finger chase, nose-finger test, fast alternating hand movements, and heel-shin slide were performed and rated by experienced and trained investigators.

2.8. Statistical analysis

Analysis of variance (ANOVA) with montage as within-subject factor and group as between-subject factor was applied to evaluate differences in electric field strength between SCA3 mutation carriers and healthy controls in each ROI. Mauchly's test was used to check the assumption of sphericity and followed by a Greenhouse-Geisser correction if necessary.

Associations between electric field strength and skin-cerebellum distance, morphometric posterior fossa features, ataxia severity, total cerebellar grey matter volume, and total cerebellar white matter volume were explored with Pearson or Spearman coefficients, if appropriate. Stepwise linear regression analyses were subsequently performed to identify factors that independently affect electric field strength. To limit the number of regression analyses, we focused on the extracephalic montage, which was used in our own and other trials (Benussi et al., 2017, Maas et al., 2022a, Maas et al., 2022b, Naeije et al., 2023, Reumers et al., 2025), and selected the midline and right-sided ROIs (i.e., ROI1 and ROI6 in the anterior and posterior vermis and ROI2, ROI4, and ROI7 in the right cerebellar hemisphere).

All statistical analyses were performed in SPSS Statistics (IBM, version 29). The Benjamini-Hochberg procedure was applied to control the false discovery rate (FDR) at 0.05.

3. Results

3.1. Demographic and clinical characteristics of participants

Sixty-eight SCA3 mutation carriers and thirty-seven healthy controls participated in this study. Age and sex were comparable between both groups (SCA3: 46.6 ± 12.3 years, 36/68 males [52.9%]; healthy controls: 47.7 ± 12.7 years, 18/37 males [48.6%]). SCA3 mutation carriers had a mean SARA score of 9.0 points (SD = 7.1 points), disease duration of 10.7 years (SD = 6.5 years), and repeat length of 67.8 (SD = 4.6). Absolute cerebellar grey matter, white matter, and brainstem volumes, as well as normalized volumes of these structures (i.e., relative to eTIV) and morphometric parameters are listed for SCA3 mutation carriers and healthy controls in Supplementary Table 1. There were no significant differences in electric field strengths and morphometric posterior fossa parameters between individuals with SCA3 from different sites (all p values > 0.24).

3.2. Electric field strength and distribution in SCA3 mutation carriers versus healthy controls

Fig. 1 presents cerebellar tDCS-induced electric field strengths in volts per meter (V/m) with a buccinator, frontopolar, and lower neck reference electrode in each of the eight selected ROIs in SCA3 mutation carriers and healthy controls. Illustrative cerebellar flatmaps of each montage are shown in Fig. 2 for a mildly, moderately, and severely affected SCA3 mutation carrier, as well as a healthy control. ANOVA revealed a significant montage × group interaction for the three ROIs in the anterior lobe (all p values < 0.001), as well as ROI6 in the posterior vermis ($p < 0.001$) and ROI8 in left lobule VIIIA ($p = 0.012$). The main effect of reference electrode position on cerebellar tDCS-induced electric field strength showed a significant difference between lower neck, buccinator, and frontopolar montages in each of the eight examined cerebellar regions (all p values < 0.001). The frontopolar montage consistently yielded the highest field strengths, while the lower neck montage caused the lowest field strengths (p values < 0.001 for all pairwise comparisons). The main effect of group showed a significant difference between SCA3 mutation carriers and healthy controls in the three anterior cerebellar regions (ROI1: $F = 9.03$, $p = 0.003$, partial $\eta^2 = 0.081$; ROI2: $F = 10.38$, $p = 0.002$, partial $\eta^2 = 0.092$; ROI3: $F = 9.27$, $p = 0.003$, partial $\eta^2 = 0.083$) and right lobule VIIIA (ROI7: $F = 5.30$, $p = 0.023$, partial $\eta^2 = 0.049$). Smaller between-group differences in other posterior cerebellar regions were no longer significant after FDR correction (ROI4: $F = 3.99$, $p = 0.048$, partial $\eta^2 = 0.037$; ROI6: $F = 4.09$, $p = 0.046$, partial $\eta^2 = 0.038$; ROI8: $F = 4.59$, $p = 0.035$, partial $\eta^2 = 0.043$). Between-group differences in electric field strength in each of the ROIs were larger for the cephalic buccinator (p range 0.001 to 0.062, Cohen's d range 0.39 to 0.69) and frontopolar montage (p range < 0.001 to 0.049, Cohen's d range 0.41 to 0.90) as compared with the extracephalic lower neck montage (p range 0.037 to 0.58, Cohen's d range

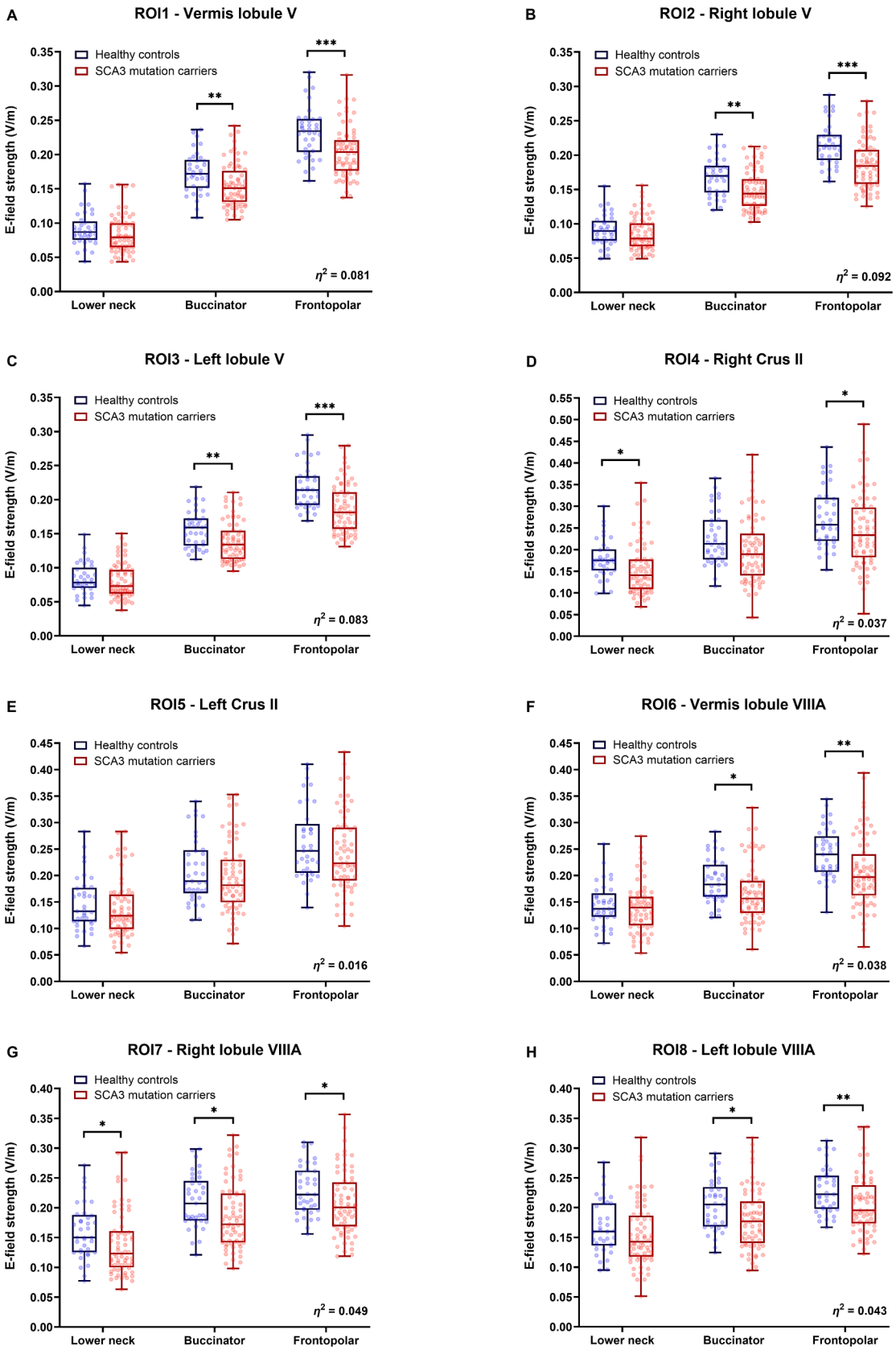

Fig. 1. Electric field strengths induced by cerebellar tDCS in each of the eight selected ROIs using different electrode montages in 68 SCA3 mutation carriers and 37 healthy controls. Whiskers represent the minimum and maximum values. The reported partial eta squared value indicates the between-group effect size in each ROI.

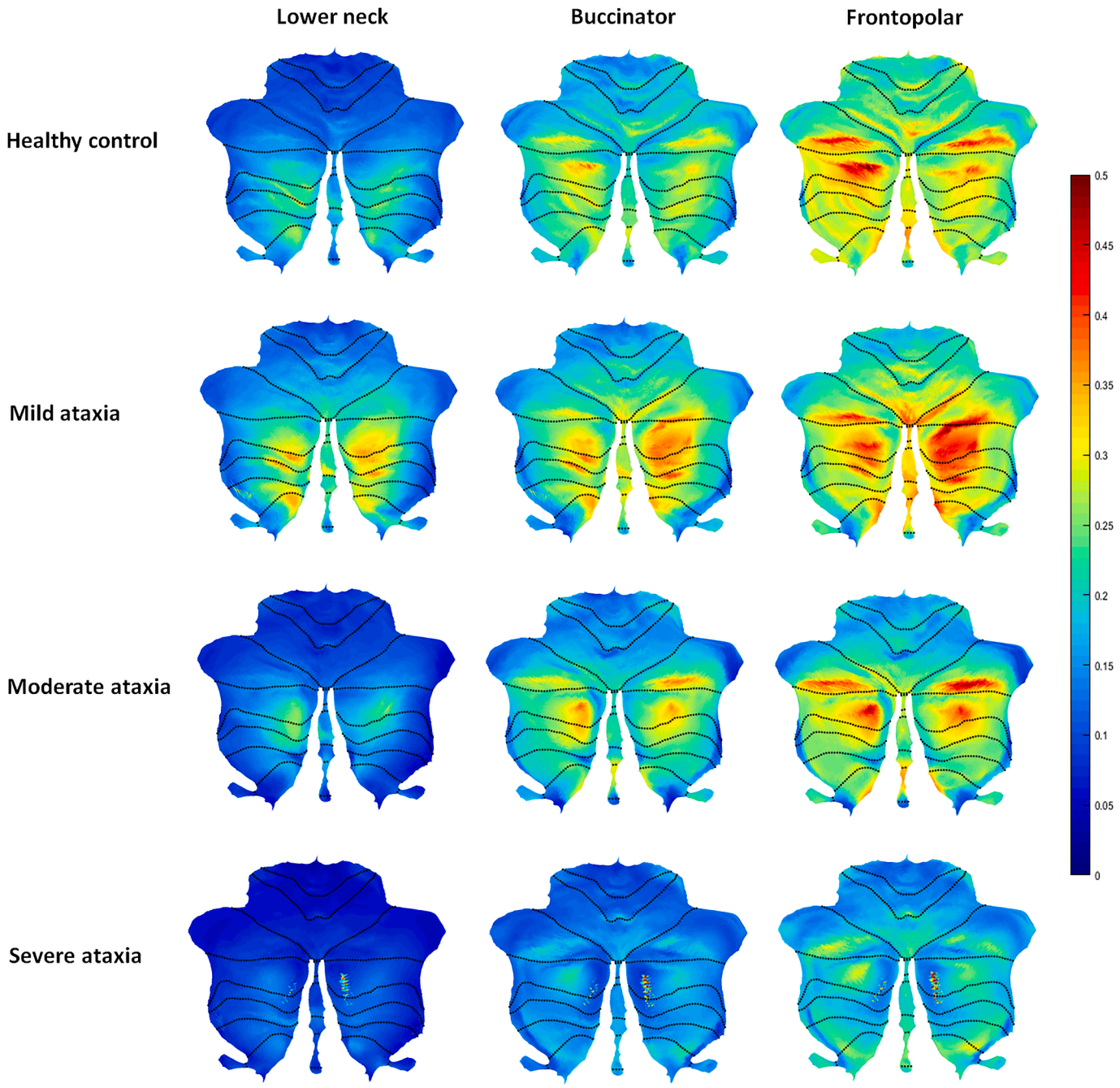

Fig. 2. Illustrative cerebellar flatmaps of the lower neck, buccinator, and frontopolar montage for a 46-year old healthy female, 48-year old mildly affected female SCA3 mutation carrier (SARA score 7), 46-year old moderately affected female SCA3 mutation carrier (SARA score 17), and 46-year old severely affected female SCA3 mutation carrier (SARA score 25.5).

0.11 to 0.43). Finally, there were significant differences in field focality between the three montages in healthy controls [F (1.22, 44.07) = 266.24, $p < 0.001$, partial $\eta^2 = 0.88$] and SCA3 mutation carriers [F (1.55, 103.63) = 256.8, $p < 0.001$, partial $\eta^2 = 0.79$]. The volume of grey matter with a field strength equal to or higher than 50% of the 99.9th percentile was highest with a frontopolar montage (healthy controls: 194.3 ± 57.7 cm^3; SCA3 mutation carriers: 152.0 ± 56.1 cm^3), followed by the buccinator montage (healthy controls: 117.2 ± 31.1 cm^3; SCA3 mutation carriers: 93.2 ± 32.3 cm^3), and lowest in the lower neck montage (healthy controls: 43.1 ± 12.6 cm^3; SCA3 mutation carriers: 42.0 ± 15.7 cm^3).

3.3. Effects of age, interindividual anatomical variability, and disease severity on electric field strength in SCA3 mutation carriers

Average field strengths in each of the ROIs were inversely associated with skin-cerebellum distance (Pearson's r range −0.61 to −0.82, all p values < 0.001, Fig. 3), SARA score (Spearman's r_s range −0.33 to −0.59, all p values < 0.006. Fig. 4), and occipital angle (r range −0.31 to −0.50, all p values < 0.006, Fig. 5). Smaller cerebellar white matter volume in SCA3 mutation carriers was associated with lower electric field strengths in part of the ROIs (frontopolar montage: r_s range 0.22 to 0.41, p range < 0.001 to 0.08; buccinator montage: r_s range 0.20 to 0.34, p range 0.005 to 0.10; lower neck montage: r_s range 0.08 to 0.35, p range 0.003 to 0.51) (Supplementary Fig. 1). No associations were found

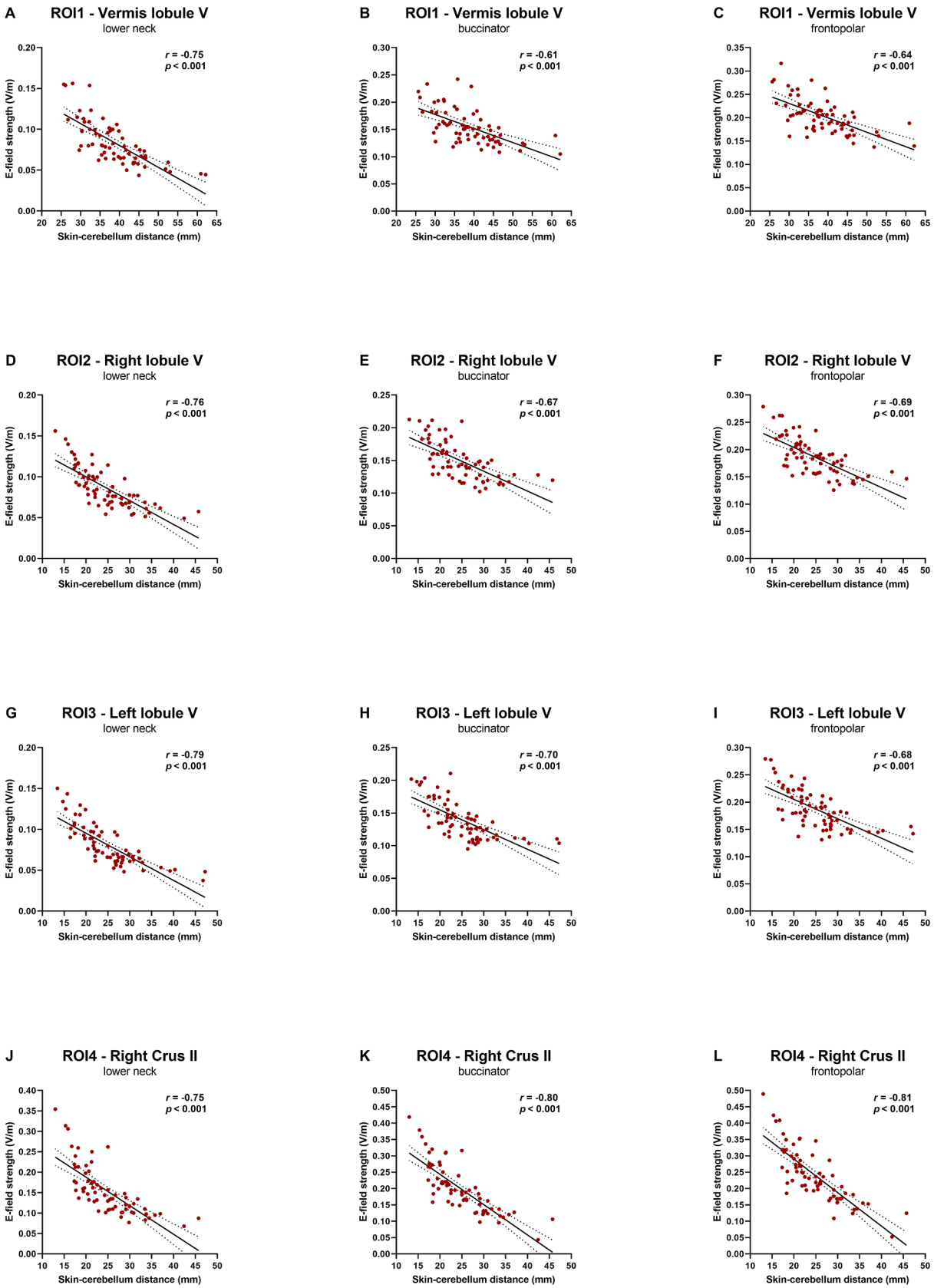

Fig. 3. Associations between cerebellar tDCS-induced electric field strength in each of the eight selected ROIs and skin-cerebellum distance in 68 SCA3 mutation carriers using a lower neck montage (A, D, G, J, M, P, S, V), buccinator montage (B, E, H, K, N, Q, T, W), and frontopolar montage (C, F, I, L, O, R, U, X).

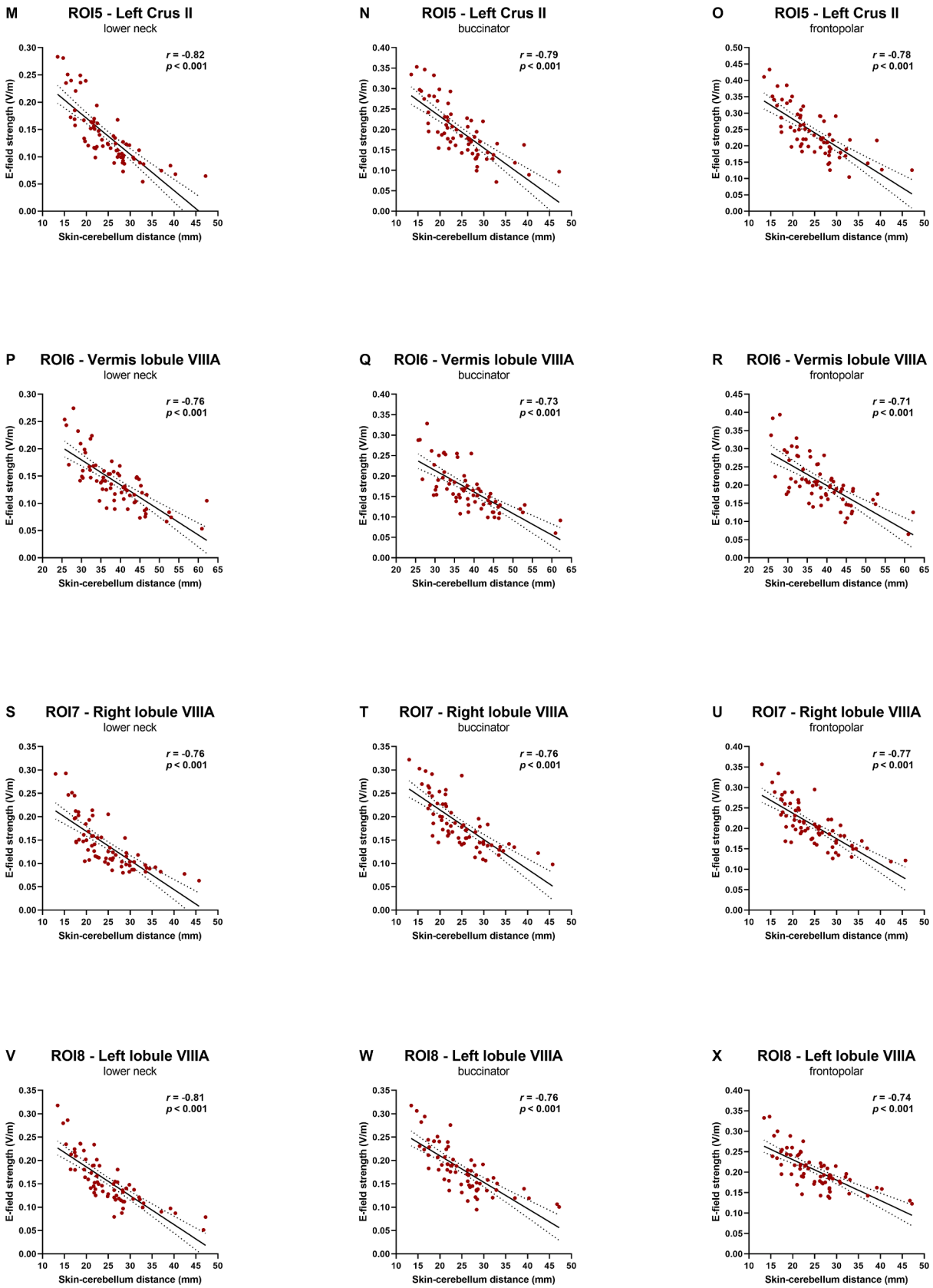

Fig. 3. (*continued*).

between electric field strength and total cerebellar grey matter volume (r range −0.02 to 0.23, all p values > 0.06), pons angle (r range −0.17 to 0.02, all p values > 0.13), cerebellar angle (r range −0.13 to −0.28, all p values > 0.02), and tentorial angle (r range 0.03 to 0.31, all p values > 0.009) in SCA3 mutation carriers.

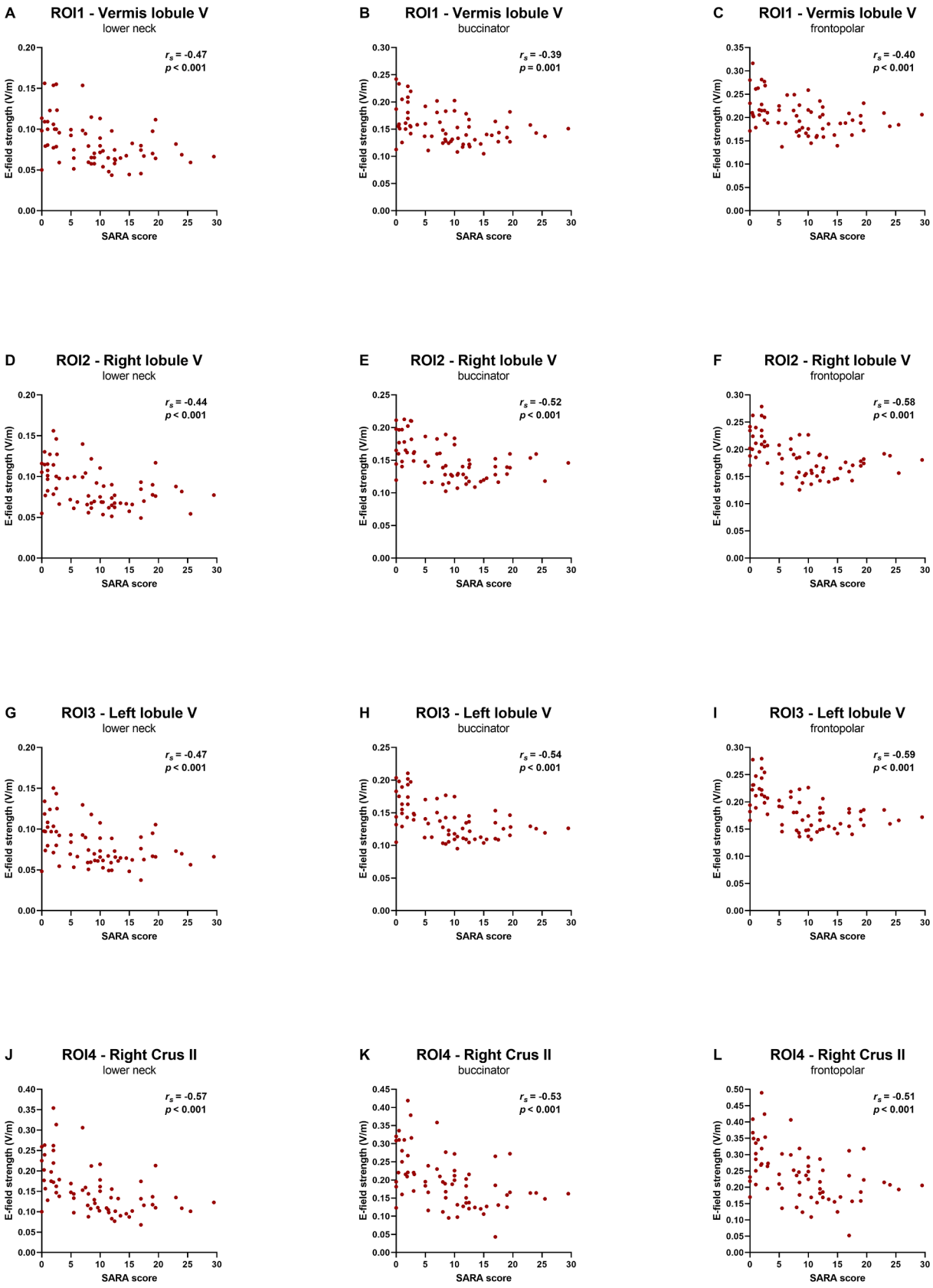

Fig. 4. Associations between cerebellar tDCS-induced electric field strength in each of the eight selected ROIs and SARA score in 68 SCA3 mutation carriers using a lower neck montage (A, D, G, J, M, P, S, V), buccinator montage (B, E, H, K, N, Q, T, W), and frontopolar montage (C, F, I, L, O, R, U, X).

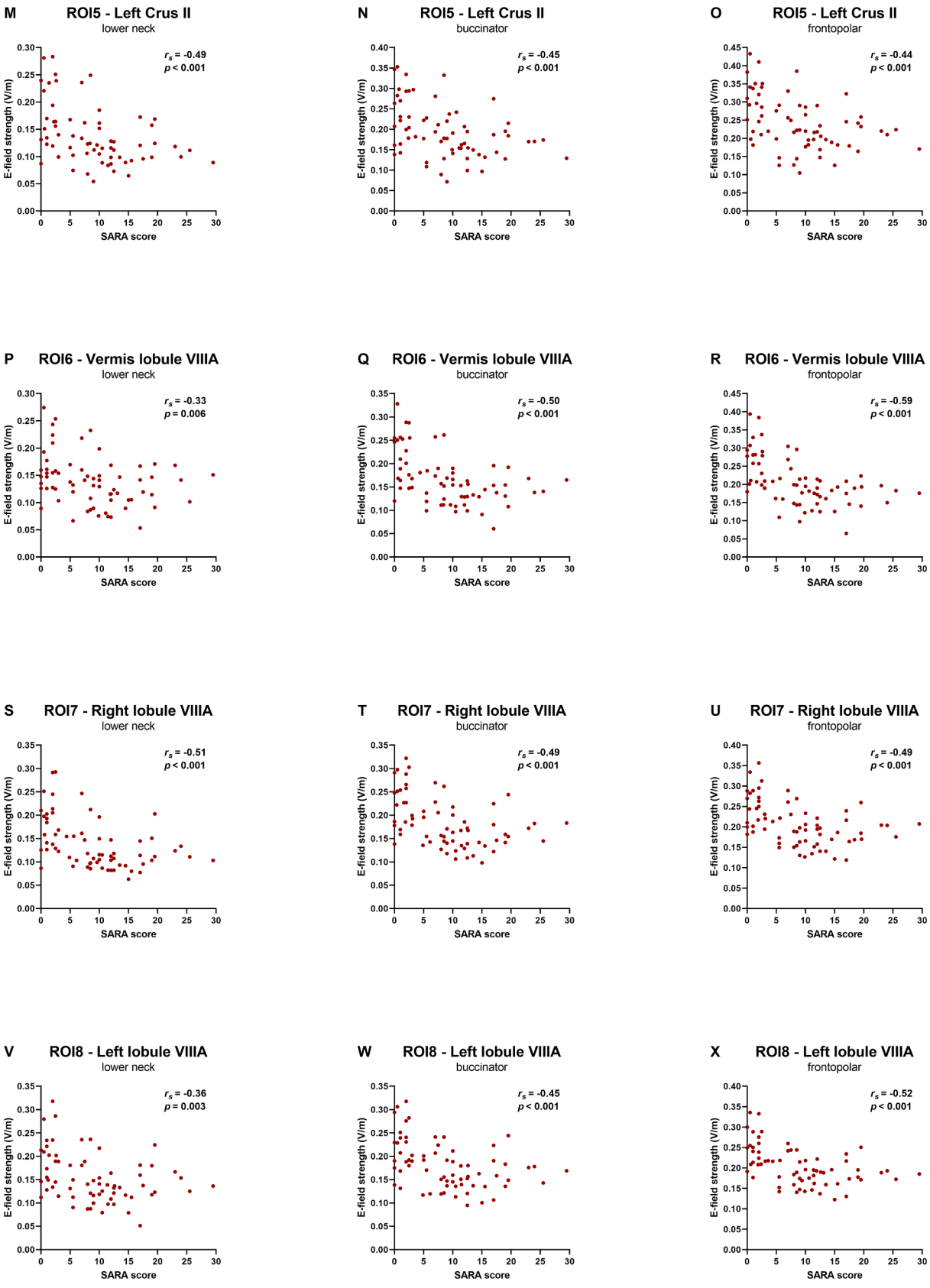

Fig. 4. (*continued*).

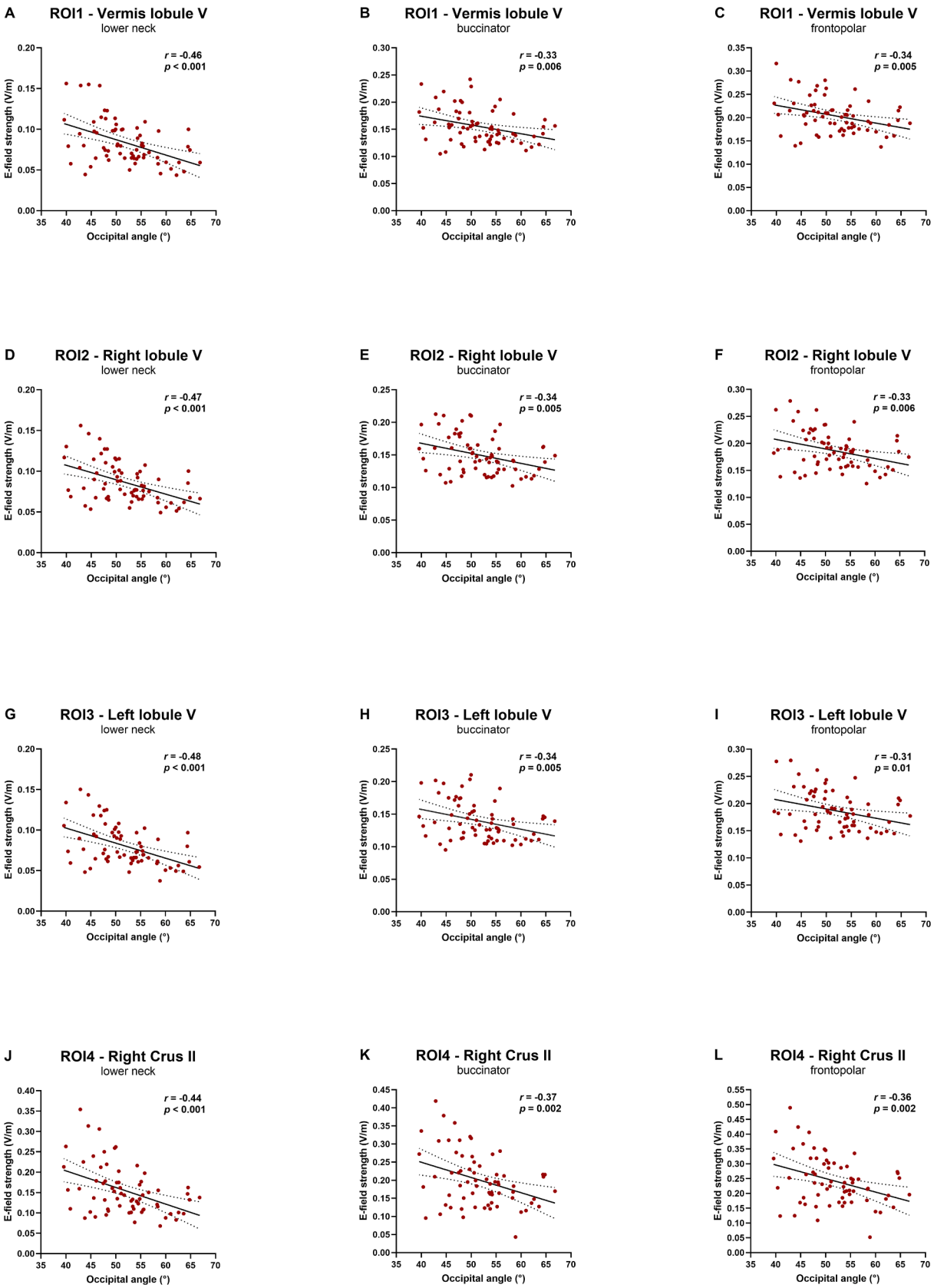

Fig. 5. Associations between cerebellar tDCS-induced electric field strength in each of the eight selected ROIs and occipital angle in 68 SCA3 mutation carriers using a lower neck montage (A, D, G, J, M, P, S, V), buccinator montage (B, E, H, K, N, Q, T, W), and frontopolar montage (C, F, I, L, O, R, U, X).

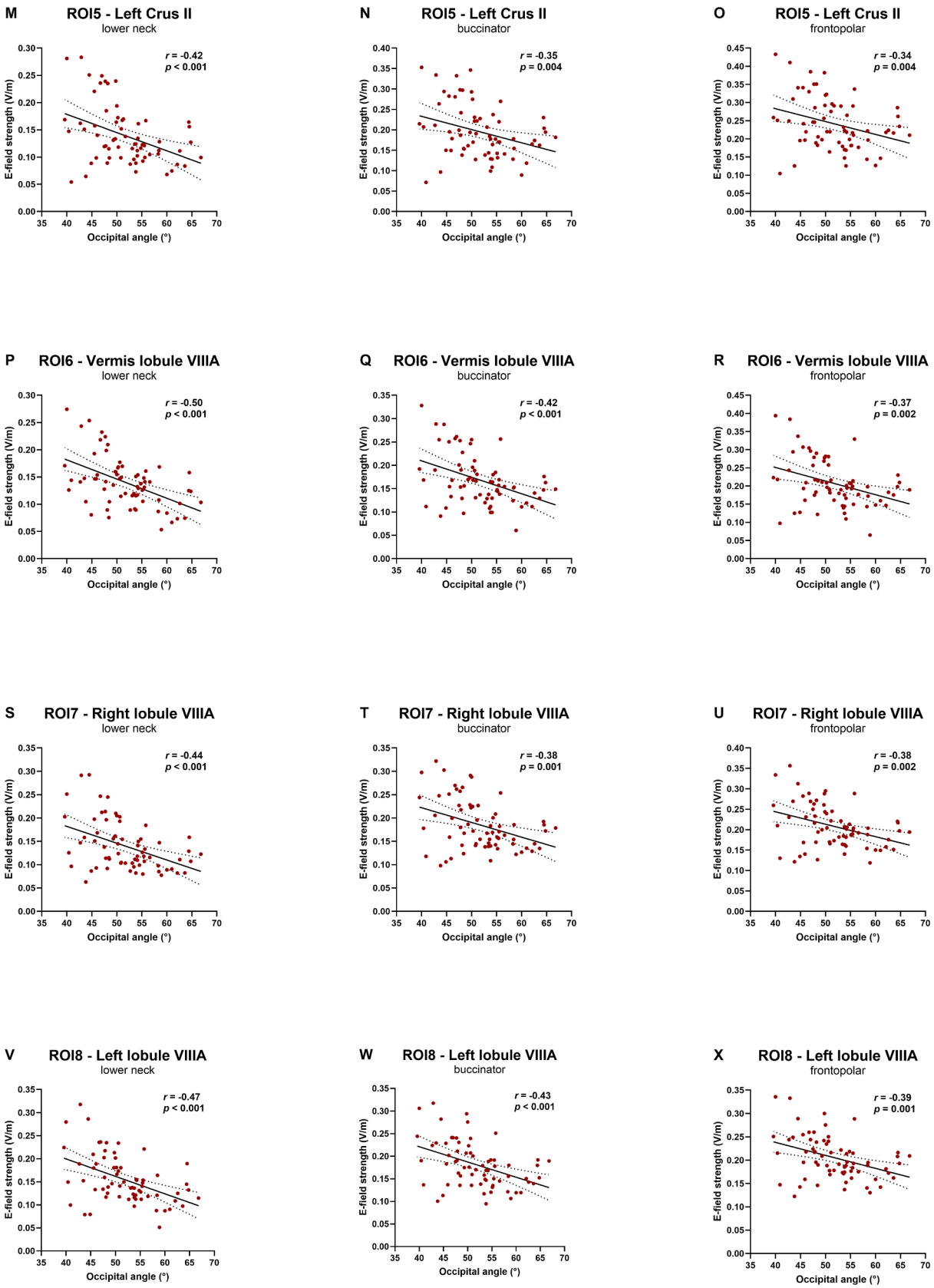

Fig. 5. (*continued*).

3.4. Independent predictors of electric field strength in SCA3 mutation carriers

Multivariable linear regression was performed to identify factors that are independently associated with electric field strength. Following the abovementioned exploratory, univariate analyses, skin-cerebellum distance, SARA score, occipital angle, and cerebellar white matter volume were selected as independent variables. Unstandardized coefficients (*b*) and their 95% confidence intervals, standardized coefficients (beta), and R^2 values are summarized in Table 1 (lower neck montage), Supplementary Table 2 (buccinator montage), and Supplementary Table 3 (frontopolar montage). Variance inflation factors in the final regression models ranged between 1.05 and 1.24, which are considered acceptable values (i.e., < 5) (Akinwande et al., 2015).

Average field strength in the anterior vermis (ROI1) and right cerebellar hemisphere (ROI2, ROI4, and ROI7) was independently associated with skin-cerebellum distance, SARA score, and occipital angle for the lower neck montage. Together, these variables accounted for 67% of the variance in electric field strength. Skin-cerebellum distance was the strongest predictor in each model, but addition of the other two variables resulted in a significant ~ 10% increase in explained variance. Electric field strength in the posterior vermis (ROI6) was independently associated with skin-cerebellum distance and occipital angle, but not SARA score. Both variables accounted for 62% of the variance in field strength.

4. Discussion

Electric field strength and distribution within the posterior fossa are proposed to play an important role in cerebellar neuromodulation with tDCS, but have so far not been examined in patients with ataxia. Leveraging high-resolution MRI scans from the ESMI cohort, we simulated cerebellar midline tDCS in SCA3 mutation carriers and examined how electric field strengths in different cerebellar regions are affected by ataxia severity, individual anatomical features, and electrode montage. The main findings of this study can be summarized as follows. First, field strengths induced by cerebellar tDCS were overall lower in individuals with SCA3 compared with healthy adults. The largest between-group difference was found in the anterior lobe. Second, similar to healthy controls, the frontopolar montage consistently produced the highest field strengths throughout the cerebellum (with the lowest field focality), and skin-cerebellum distance emerged as the most important underlying parameter. Third, ataxia severity and occipital angle were found to be additional predictors of tDCS-induced field strength in SCA3.

Despite considerable interindividual variability in electric field strengths, especially in the posterior lobe, differences were observed throughout the cerebellum between SCA3 mutation carriers and healthy controls. Effect sizes were medium to large for ROIs in the anterior lobe (which predominantly regulates motor functions) versus small to medium for ROIs in the posterior lobe (which predominantly regulates non-motor functions). Smaller differences with healthy controls and highest field strengths in the (more superficially located) posterior lobe could lead to the hypothesis that tDCS effects might be larger for cognitive and emotional dysfunction than for motor deficits. However, in the only trial so far that primarily focused on cognitive performance, Reumers and colleagues recently reported a significant decrease in ataxia severity in a mixed sample of patients with degenerative ataxias and cerebellar strokes but no improvement of executive functioning (Reumers et al., 2025). Further studies are warranted in etiologically homogeneous populations, also to evaluate associations between clinical changes and electric field strengths.

When applying cerebellar midline tDCS, our modelling data show that placement of the reference electrode over the frontopolar region produced the highest field strengths throughout the cerebellum. Whether this also translates into more pronounced physiological, behavioural, or clinical outcomes requires further investigation. At the same time, the clinical implications of a more extensive extracerebellar current distribution, also involving the frontal and temporal lobes, remain unknown. In addition to progressive motor impairment, patients with cerebellar disorders including SCA3 commonly experience cognitive and affective symptoms (Hoche et al., 2018, Maas et al., 2021, Reumers et al., 2024, Schmahmann and Sherman, 1998). These are thought to result from altered connectivity between the cerebellar cortex and prefrontal, posterior parietal, superior temporal, and paralimbic cortices (Schmahmann et al., 2019). Given the widespread cerebellar-cerebral connections, we cannot exclude the possibility that spread of currents to these extracerebellar regions induced by a frontopolar montage also affects non-motor symptoms. Finally, possible differences in tolerability and blinding efficacy between montages should be taken into account in the design of future trials. Compared with extracranial references electrodes, a frontopolar montage may be associated with stronger physical sensations and higher discomfort due to a thinner skin and higher density of cutaneous nerves on the forehead.

In line with modelling research in healthy adults (Gomez-Tames et al., 2019, Klaus and Schutter, 2021, Maas et al., 2023), we showed that skin-cerebellum distance is the main variable determining cerebellar tDCS-induced electric field strength in SCA3 mutation carriers. The present data indicate that approximately 50–60% of the variance in field strength in SCA3 mutation carriers is explained by this parameter, which is comparable to healthy adults. Interindividual differences in posterior fossa morphometry were previously found to account for another 10% of variance in healthy volunteers (Maas et al., 2023).

Table 1
Predictors of cerebellar tDCS-induced electric field strength in five selected ROIs in 68 SCA3 mutation carriers using a lower neck montage. Skin-cerebellum distance, Scale for the Assessment and Rating of Ataxia (SARA) score, occipital angle, and cerebellar white matter volume were chosen as independent variables.

	Predictors	R^2	ΔR^2	B	95% CI	Beta	*P* value
ROI1	1. Skin-cerebellum distance	0.66	0.1	−0.002	−0.003; −0.002	−0.62	< 0.001
	2. SARA score			−0.001	−0.002; 0.00	−0.27	< 0.001
	3. Occipital angle			−0.001	−0.001; 0.00	−0.17	0.044
ROI2	1. Skin-cerebellum distance	0.67	0.09	−0.002	−0.003; −0.002	−0.63	< 0.001
	2. Occipital angle			−0.001	−0.002; 0.00	−0.26	< 0.001
	3. SARA score			−0.001	−0.001; 0.00	−0.15	0.049
ROI4	1. Skin-cerebellum distance	0.67	0.11	−0.005	−0.007; −0.004	−0.59	< 0.001
	2. SARA score			−0.002	−0.004; −0.001	−0.27	< 0.001
	3. Occipital angle			−0.002	−0.004; −0.001	−0.23	0.003
ROI6	1. Skin-cerebellum distance	0.62	0.04	−0.004	−0.005; −0.003	−0.67	< 0.001
	2. Occipital angle			−0.002	−0.003; 0.00	−0.23	0.008
ROI7	1. Skin-cerebellum distance	0.67	0.09	−0.005	−0.006; −0.004	−0.62	< 0.001
	2. Occipital angle			−0.002	−0.003; −0.001	−0.23	0.003
	3. SARA score			−0.002	−0.003; 0.00	−0.21	0.009

B = unstandardized coefficient, beta = standardized coefficient, CI = confidence interval, ΔR^2 = change in R^2 compared with a model that only includes skin-cerebellum distance.

Specifically, larger pons angles and smaller cerebellar angles were associated with larger field strengths within the cerebellar cortex. In the present study, we were unable to replicate this finding in SCA3 mutation carriers, possibly due to differences in cerebellopontine structure in a neurodegenerative disorder. Notably, the occipital angle, which was associated with electric field strength in several ROIs in univariate analyses in healthy controls but not retained in multivariable linear regression models, turned out to be an independent predictor of electric field strength in SCA3 mutation carriers.

The association between tDCS-induced field strength at the cerebellar cortical surface and ataxia severity is an important observation of this study. It indicates that higher current intensities are required in more severely affected patients to reach a similar electric field strength at the target site. As a functional measure, SARA score serves as a surrogate for the anatomical and pathophysiological changes that affect current flow. These underlying biological mechanisms might relate to gradually progressive cerebellar and brainstem atrophy, skin-cerebellum distance, other as yet undefined anatomical factors, or a complex interplay between them, and warrant further examination in future tDCS studies that integrate high-resolution neuroimaging, electric field modelling, and (non-)motor outcomes. From a clinical perspective, improvements in ataxia severity with a fixed current intensity of 2 mA were most pronounced in patients with lower SARA scores (Benussi et al., 2018, Benussi et al., 2017). Although cerebellar volumes were not reported and patient samples were etiologically heterogeneous, it is likely that these individuals had the least severe disruption of cerebellar circuitry and/or cerebellar atrophy. The parallel between these empirical clinical findings and our theoretical modelling work arguably supports the relevance of evaluating field strengths in cerebellar patients, aligns with the cerebellar reserve hypothesis (Manto et al., 2021, Mitoma et al., 2020), and suggests that individualized dosing might increase the efficacy of cerebellar tDCS. However, in addition to absolute electric field magnitudes, the therapeutic potential of repeated cerebellar tDCS sessions to induce longer-lasting, plasticity-related changes depends on a complex, as yet largely undefined interaction of numerous factors, at least including (i) the number of preserved cerebellar neurons effectively exposed to a sufficient electric field, (ii) the specific orientation of these neurons in the highly convoluted cerebellar cortex with respect to the current flow, (iii) the duration, number, and repetition frequency of tDCS sessions, and (iv) functional brain state (Benussi et al., 2023). Stronger field strengths may be relevant for immediate neurophysiological changes, but the dose–response relationship is not necessarily linear and can plateau or even reverse (Batsikadze et al., 2013).

A recently published post-hoc analysis from a randomized, sham-controlled, single-blind cross-over trial in Friedreich ataxia revealed that clinical effects of cerebellar tDCS were related to cerebellar volume (Naeije et al., 2025), supporting the notion that an individual's cerebellar anatomy matters (Maas and Schutter, 2025). Patients with larger grey matter volumes of the anterior and posterior lobe, as segmented with the CERES pipeline of volBrain (Romero et al., 2017), were more likely to exhibit motor and non-motor improvements, respectively, when compared to individuals with smaller volumes. Using CerebNet (Faber et al., 2022), our modelling study showed an association between (lower) cerebellar tDCS-induced electric field strengths and (smaller) cerebellar white matter volume, but not cerebellar grey matter volume, in SCA3 mutation carriers. We hypothesize that these univariate associations may have been due to an extension of the 5-mm radius spherical ROIs into the cerebellar white matter. Indeed, there is increasing evidence that cerebellar white matter damage is part of the pathophysiology of SCA3 and related to ataxia severity (Ferreira et al., 2024, Putka et al., 2023).

Strengths of the present study were the inclusion of a large number of SCA3 mutation carriers in different disease stages, the evaluation of three commonly used reference electrode positions, and the selection of multiple ROIs in functionally diverse parts of the cerebellum. While the modelling methodology builds on established work, the application to a neurodegenerative ataxia population is novel and clinically important. Several limitations of this study should also be discussed. The main limitation resides in its computational modelling nature without direct clinical correlates to test the relevance of the predicted between-subject differences. Inspired by associations between tDCS-induced field strength in supratentorial brain regions and clinical outcomes in patients with psychiatric disorders (Mondino et al., 2021, Suen et al., 2021, Yachou et al., 2025), we primarily provide a theoretical framework for explaining (part of) the observed heterogeneity in treatment response to cerebellar tDCS across SCA3 patients (Maas et al., 2022b). Future tDCS studies are needed to explore associations between the predicted field strength in a target region and the actually observed clinical and neurophysiological effects. Second, we acknowledge that certain aspects of real-world tDCS application are difficult to capture comprehensively with computational modelling approaches. For instance, the simplified assumption of perfect skin contact in simulation studies might lead to a systematic overestimation of electric field strengths at the target site, of which the exact extent remains unknown. Third, although we excluded gross segmentation errors with visual inspection, residual deviations could have affected the precision of the field simulations (Puonti et al., 2020). Fourth, the assumption of uniform tissue conductivity values in electric field modelling (Rezaee and Dutta, 2019, Wagner et al., 2004, Windhoff et al., 2013) disregards real-world anisotropy in cerebellar white matter and might therefore underestimate tangential currents along fiber tracts. Moreover, white matter damage in neurodegenerative diseases, such as SCA3, could introduce differences in conductivity. Further modelling work might benefit from incorporating diffusion-weighted imaging sequences, which will allow more accurate estimates, and pathology-adjusted values. Fifth, the use of fixed spherical ROIs based on MNI coordinates that have been transformed to subject space may not fully capture interindividual anatomical differences, especially in patients with advanced cerebellar atrophy. Considering individualized lobular labels to ensure that only grey matter is included in regions of interest may further improve the precision of electric field simulations in the cerebellum. Sixth, as MRI scans in ESMI did not cover the entire spinal cord, we were unable to include the cerebello-spinal montage in this modelling study.

In conclusion, our data indicate that skin-cerebellum distance, ataxia severity, and morphometric posterior fossa parameters are associated with the magnitude of cerebellar tDCS-induced electric fields in SCA3, explaining up to 70% of variance. Interindividual differences in field strength at the target site despite similar electrode positions and current intensity might eventually set the stage for personalized neuromodulation protocols in cerebellar diseases. Our findings also provide evidence that montage selection significantly influences the magnitude and spatial pattern of the electric field induced by cerebellar midline tDCS. Although additional studies are required to empirically link differences in field strength to interindividual variability in clinical outcomes, one may consider to already take these factors into account when designing cerebellar tDCS trials in patients with degenerative ataxias.

Author contributions

Roderick Maas obtained funding from the National Ataxia Foundation to perform this substudy of ESMI, designed the tDCS modelling project, analyzed and interpreted the data, and drafted the manuscript. Jennifer Faber was responsible for the monitoring and export of ESMI data and commented on the draft version. Bart van de Warrenburg contributed to the design of the project and commented on the draft version. Dennis Schutter contributed to the design of the project and data interpretation and commented on the draft version.

Funding

This study was funded by the National Ataxia Foundation and used data from ESMI, an EU Joint Programme – Neurodegenerative Disease Research (JPND) project (see https://www.jpnd.eu). ESMI is supported through the following funding organisations under the aegis of JPND: Germany, Federal Ministry of Education and Research (BMBF; funding codes 01ED1602A/B); Netherlands, The Netherlands Organisation for Health Research and Development; Portugal, Foundation for Science and Technology and Regional Fund for Science and Technology of the Azores; United Kingdom, Medical Research Council. ESMI has received funding from the European Union's Horizon 2020 research and innovation programme under grant agreement No 643417. At the US sites, ESMI was in part supported by the National Ataxia Foundation and the National Institute of Neurological Disorders and Stroke (NINDS) grant R01NS080816.

Declaration of competing interest

Roderick Maas receives research support from the National Ataxia Foundation, Ataxia UK, Friedreich's Ataxia Research Alliance, and Stichting Friedreich Ataxie Nederland. Jennifer Faber was funded within the Advanced Clinician Scientist Programme (ACCENT, funding code 01EO2107) by the German Federal Ministry of Education and Research (BMBF) and as a PI of the iBehave Network, sponsored by the Ministry of Culture and Science of the State of North Rhine-Westphalia, and received funding from the National Ataxia Foundation and consultancy honoraria from Vico Therapeutics and Biogen. Bart van de Warrenburg receives research support from ZonMw, Dutch Scientific Organization, Hersenstichting, Gossweiler Foundation, and Christina Foundation, receives royalties from BSL – Springer Nature, and has served on a scientific advisory board of / did paid consultancy for Biohaven, Biogen, and Vico Therapeutics. Dennis Schutter receives research support from the Dutch Research Foundation (NWO, VI.C.181.005).

Appendix

ESMI MR Study Group contributors: Paola Giunti (Ataxia Centre, Department of Clinical and Movement Neurosciences, UCL Queen Square Institute of Neurology, University College London, London, United Kingdom), Thomas Klockgether (German Center for Neurodegenerative Diseases [DZNE], Bonn, Germany), Khalaf Bushara (Ataxia Center, Department of Neurology, University of Minnesota, Minneapolis, USA), Dagmar Timmann (Department of Neurology and Center for Translational Neuro- and Behavioral Sciences [C-TNBS], Essen University Hospital, University of Duisburg-Essen, Essen, Germany), Kathrin Reetz (Department of Neurology, RWTH Aachen University, and JARA-BRAIN Institute Molecular Neuroscience and Neuroimaging, Forschungszentrum Jülich GmbH and RWTH Aachen University, Aachen, Germany), Heike Jacobi (Department of Neurology, University Hospital Heidelberg, Heidelberg, Germany), Chiadi Onyike (Department of Psychiatry and Behavioral Sciences, Johns Hopkins University School of Medicine, Baltimore, USA).

Appendix A. Supplementary data

Supplementary data to this article can be found online at https://doi.org/10.1016/j.clinph.2025.2111405.

References

Akinwande, M.O., Dikko, H.G., Samson, A., 2015. Variance inflation factor: As a Condition for the Inclusion of Suppressor Variable(s) in Regression Analysis. Open J. Stat. 05 (07), 754–767. https://doi.org/10.4236/ojs.2015.57075.

Antonenko, D., Thielscher, A., Saturnino, G.B., Aydin, S., Ittermann, B., Grittner, U., et al., 2019. Towards precise brain stimulation: is electric field simulation related to neuromodulation? Brain Stimul. 12 (5), 1159–1168. https://doi.org/10.1016/j.brs.2019.03.072.

Batsikadze, G., Moliadze, V., Paulus, W., Kuo, M.F., Nitsche, M.A., 2013. Partially non-linear stimulation intensity-dependent effects of direct current stimulation on motor cortex excitability in humans. J. Physiol. 591 (7), 1987–2000. https://doi.org/10.1113/jphysiol.2012.249730.

Benussi, A., Batsikadze, G., Franca, C., Cury, R.G., Maas, R.P.P.W.M., 2023. The Therapeutic potential of Non-Invasive and Invasive Cerebellar Stimulation Techniques in Hereditary Ataxias. Cells 12(8):1193. https://doi.org/10.3390/cells12081193.

Benussi, A., Dell'Era, V., Cantoni, V., Bonetta, E., Grasso, R., Manenti, R., et al., 2018. Cerebello-spinal tDCS in ataxia: a randomized, double-blind, sham-controlled, crossover trial. Neurology 91 (12), e1090–e1101. https://doi.org/10.1212/WNL.0000000000006210.

Benussi, A., Dell'Era, V., Cotelli, M.S., Turla, M., Casali, C., Padovani, A., et al., 2017. Long term clinical and neurophysiological effects of cerebellar transcranial direct current stimulation in patients with neurodegenerative ataxia. Brain Stimul. 10 (2), 242–250. https://doi.org/10.1016/j.brs.2016.11.001.

Faber, J., Kugler, D., Bahrami, E., Heinz, L.S., Timmann, D., Ernst, T.M., et al., 2022. CerebNet: a fast and reliable deep-learning pipeline for detailed cerebellum sub-segmentation. Neuroimage 264, 119703. https://doi.org/10.1016/j.neuroimage.2022.119703.

Ferreira, M., Schaprian, T., Kugler, D., Reuter, M., Deike-Hoffmann, K., Timmann, D., et al., 2024. Cerebellar Volumetry in Ataxias: Relation to Ataxia Severity and Duration. Cerebellum 23 (4), 1521–1529. https://doi.org/10.1007/s12311-024-01659-0.

Gomez-Tames, J., Asai, A., Mikkonen, M., Laakso, I., Tanaka, S., Uehara, S., et al., 2019. Group-level and functional-region analysis of electric-field shape during cerebellar transcranial direct current stimulation with different electrode montages. J. Neural Eng. 16 (3), 036001. https://doi.org/10.1088/1741-2552/ab0ac5.

Hoche, F., Guell, X., Vangel, M.G., Sherman, J.C., Schmahmann, J.D., 2018. The cerebellar cognitive affective/Schmahmann syndrome scale. Brain 141 (1), 248–270. https://doi.org/10.1093/brain/awx317.

Jurcak, V., Tsuzuki, D., Dan, I., 2007. 10/20, 10/10, and 10/5 systems revisited: their validity as relative head-surface-based positioning systems. Neuroimage 34 (4), 1600–1611. https://doi.org/10.1016/j.neuroimage.2006.09.024.

King, M., Hernandez-Castillo, C.R., Poldrack, R.A., Ivry, R.B., Diedrichsen, J., 2019. Functional boundaries in the human cerebellum revealed by a multi-domain task battery. Nat. Neurosci. 22 (8), 1371–1378. https://doi.org/10.1038/s41593-019-0436-x.

Klaus, J., Schutter, D.J.L.G., 2021. Electrode montage-dependent intracranial variability in electric fields induced by cerebellar transcranial direct current stimulation. Sci. Rep. 11 (1), 22183. https://doi.org/10.1038/s41598-021-01755-9.

Laakso, I., Mikkonen, M., Koyama, S., Hirata, A., Tanaka, S., 2019. Can electric fields explain inter-individual variability in transcranial direct current stimulation of the motor cortex? Sci. Rep. 9 (1), 626. https://doi.org/10.1038/s41598-018-37226-x.

Maas, R.P.P.W.M., Faber, J., ESMI MR Study Group, van de Warrenburg, B.P.C., Schutter, D.J.L.G., 2023. Interindividual differences in posterior fossa morphometry affect cerebellar tDCS-induced electric field strength. Clin. Neurophysiol. 153, 152–165. https://doi.org/10.1016/j.clinph.2023.06.019.

Maas, R.P.P.W.M., Helmich, R.C.G., van de Warrenburg, B.P.C., 2020. The role of the cerebellum in degenerative ataxias and essential tremor: Insights from noninvasive modulation of cerebellar activity. Mov. Disord. 35 (2), 215–227. https://doi.org/10.1002/mds.27919.

Maas, R.P.P.W.M., Killaars, S., van de Warrenburg, B.P.C., Schutter, D.J.L.G., 2021. The cerebellar cognitive affective syndrome scale reveals early neuropsychological deficits in SCA3 patients. J. Neurol. 268 (9), 3456–3466. https://doi.org/10.1007/s00415-021-10516-7.

Maas, R.P.P.W.M., Schutter, D.J.L.G., 2025. Cerebellar transcranial direct current stimulation in Friedreich ataxia: Anatomy matters. Clin. Neurophysiol. 2110784. https://doi.org/10.1016/j.clinph.2025.2110784.

Maas, R.P.P.W.M., Schutter, D.J.L.G., Toni, I., Timmann, D., van de Warrenburg, B.P.C., 2022a. Cerebellar transcranial direct current stimulation modulates timing but not acquisition of conditioned eyeblink responses in SCA3 patients. Brain Stimul. 15 (3), 806–813. https://doi.org/10.1016/j.brs.2022.05.013.

Maas, R.P.P.W.M., Teerenstra, S., Toni, I., Klockgether, T., Schutter, D., van de Warrenburg, B.P.C., 2022b. Cerebellar Transcranial Direct Current Stimulation in Spinocerebellar Ataxia Type 3: a Randomized, Double-blind, Sham-Controlled Trial. Neurotherapeutics 19 (4), 1259–1272. https://doi.org/10.1007/s13311-022-01231-w.

Manto, M., Kakei, S., Mitoma, H., 2021. The critical need to develop tools assessing cerebellar reserve for the delivery and assessment of non-invasive cerebellar stimulation. Cerebellum Ataxias 8 (1), 2. https://doi.org/10.1186/s40673-020-00126-w.

Miterko, L.N., Baker, K.B., Beckinghausen, J., Bradnam, L.V., Cheng, M.Y., Cooperrider, J., et al., 2019. Consensus Paper: Experimental Neurostimulation of the Cerebellum. Cerebellum 18 (6), 1064–1097. https://doi.org/10.1007/s12311-019-01041-5.

Mitoma, H., Buffo, A., Gelfo, F., Guell, X., Fuca, E., Kakei, S., et al., 2020. Consensus paper. cerebellar reserve: from cerebellar physiology to cerebellar disorders. Cerebellum 19 (1), 131–153. https://doi.org/10.1007/s12311-019-01091-9.

Mondino, M., Fonteneau, C., Simon, L., Donde, C., Haesebaert, F., Poulet, E., et al., 2021. Advancing clinical response characterization to frontotemporal transcranial direct current stimulation with electric field distribution in patients with schizophrenia and auditory hallucinations: a pilot study. Eur. Arch. Psychiatry Clin. Neurosci. 271 (1), 85–92. https://doi.org/10.1007/s00406-020-01149-4.

Mosayebi-Samani, M., Jamil, A., Salvador, R., Ruffini, G., Haueisen, J., Nitsche, M.A., 2021. The impact of individual electrical fields and anatomical factors on the neurophysiological outcomes of tDCS: a TMS-MEP and MRI study. Brain Stimul. 14 (2), 316–326. https://doi.org/10.1016/j.brs.2021.01.016.

Naeije, G., Georgiev, C., Cabaraux, P., Bourguignon, M., 2025. Cerebellar grey matter volume predicts cerebellar tDCS efficacy in individuals with Friedreich ataxia. Clin. Neurophysiol. 2110744. https://doi.org/10.1016/j.clinph.2025.2110744.

Naeije, G., Rovai, A., Destrebecq, V., Trotta, N., De Tiege, X., 2023. Anodal Cerebellar Transcranial Direct Current Stimulation Reduces Motor and Cognitive Symptoms in Friedreich's Ataxia: a Randomized. Sham-Controlled Trial. Mov Disord 38 (8), 1443–1450. https://doi.org/10.1002/mds.29453.

Nandi, T., Puonti, O., Clarke, W.T., Nettekoven, C., Barron, H.C., Kolasinski, J., et al., 2022. tDCS induced GABA change is associated with the simulated electric field in M1, an effect mediated by grey matter volume in the MRS voxel. Brain Stimul. 15 (5), 1153–1162. https://doi.org/10.1016/j.brs.2022.07.049.

Parazzini, M., Rossi, E., Ferrucci, R., Liorni, I., Priori, A., Ravazzani, P., 2014. Modelling the electric field and the current density generated by cerebellar transcranial DC stimulation in humans. Clin. Neurophysiol. 125 (3), 577–584. https://doi.org/10.1016/j.clinph.2013.09.039.

Puonti, O., Van Leemput, K., Saturnino, G.B., Siebner, H.R., Madsen, K.H., Thielscher, A., 2020. Accurate and robust whole-head segmentation from magnetic resonance images for individualized head modeling. Neuroimage 219, 117044. https://doi.org/10.1016/j.neuroimage.2020.117044.

Putka, A.F., Mato, J.P., McLoughlin, H.S., 2023. Myelinating Glia: potential Therapeutic Targets in Polyglutamine Spinocerebellar Ataxias. Cells 12 (4). https://doi.org/10.3390/cells12040601.

Rampersad, S.M., Janssen, A.M., Lucka, F., Aydin, U., Lanfer, B., Lew, S., et al., 2014. Simulating transcranial direct current stimulation with a detailed anisotropic human head model. IEEE Trans. Neural Syst. Rehabil. Eng. 22 (3), 441–452. https://doi.org/10.1109/TNSRE.2014.2308997.

Reumers, S.F.I., Maas, R.P.P.W.M., Schutter, D.J.L.G., Teerenstra, S., Kessels, R.P.C., de Leeuw, F.E., et al., 2025. Cerebellar Transcranial Direct Current Stimulation in the Cerebellar Cognitive Affective Syndrome: a Randomized, Double-blind, Sham-Controlled Trial. Mov. Disord. 40 (1), 121–131. https://doi.org/10.1002/mds.30043.

Reumers, S.F.I., Schutter, D.J.L.G., Maas, R.P.P.W.M., de Leeuw, F.E., Kessels, R.P.C., van de Warrenburg, B.P.C., 2024. Cognitive complaints and their impact on daily life in patients with degenerative cerebellar disorders. Cerebellum 23 (3), 1042–1052. https://doi.org/10.1007/s12311-023-01607-4.

Rezaee, Z., Dutta, A., 2019. Cerebellar lobules optimal stimulation (CLOS): a computational pipeline to optimize cerebellar lobule-specific electric field distribution. Front. Neurosci. 13, 266. https://doi.org/10.3389/fnins.2019.00266.

Romero, J.E., Coupe, P., Giraud, R., Ta, V.T., Fonov, V., Park, M.T.M., et al., 2017. CERES: a new cerebellum lobule segmentation method. Neuroimage 147, 916–924. https://doi.org/10.1016/j.neuroimage.2016.11.003.

Saturnino GB, Puonti O, Nielsen JD, Antonenko D, Madsen KH, Thielscher A. SimNIBS 2.1: A Comprehensive Pipeline for Individualized Electric Field Modelling for Transcranial Brain Stimulation. In: Makarov S, Horner M, Noetscher G, editors. Brain and Human Body Modeling: Computational Human Modeling at EMBC 2018. Cham (CH); 2019. p. 3-25.

Schmahmann, J.D., 2019. The cerebellum and cognition. Neurosci. Lett. 688, 62–75. https://doi.org/10.1016/j.neulet.2018.07.005.

Schmahmann, J.D., Guell, X., Stoodley, C.J., Halko, M.A., 2019. The theory and neuroscience of cerebellar cognition. Annu. Rev. Neurosci. 42, 337–364. https://doi.org/10.1146/annurev-neuro-070918-050258.

Schmahmann, J.D., Sherman, J.C., 1998. The cerebellar cognitive affective syndrome. Brain 121 (Pt 4), 561–579. https://doi.org/10.1093/brain/121.4.561.

Schmitz-Hubsch, T., Tezenas du Montcel, S., Baliko, L., Berciano, J., Boesch, S., Depondt, C., et al., 2006. Scale for the assessment and rating of ataxia: development of a new clinical scale. Neurology 66 (11), 1717–1720. https://doi.org/10.1212/01.wnl.0000219042.60538.92.

Stoodley, C.J., MacMore, J.P., Makris, N., Sherman, J.C., Schmahmann, J.D., 2016. Location of lesion determines motor vs. cognitive consequences in patients with cerebellar stroke. Neuroimage Clin 12, 765–775. https://doi.org/10.1016/j.nicl.2016.10.013.

Stoodley, C.J., Schmahmann, J.D., 2010. Evidence for topographic organization in the cerebellum of motor control versus cognitive and affective processing. Cortex 46 (7), 831–844. https://doi.org/10.1016/j.cortex.2009.11.008.

Suen, P.J.C., Doll, S., Batistuzzo, M.C., Busatto, G., Razza, L.B., Padberg, F., et al., 2021. Association between tDCS computational modeling and clinical outcomes in depression: data from the ELECT-TDCS trial. Eur. Arch. Psychiatry Clin. Neurosci. 271 (1), 101–110. https://doi.org/10.1007/s00406-020-01127-w.

Wagner, T.A., Zahn, M., Grodzinsky, A.J., Pascual-Leone, A., 2004. Three-dimensional head model simulation of transcranial magnetic stimulation. I.E.E.E. Trans. Biomed. Eng. 51 (9), 1586–1598. https://doi.org/10.1109/TBME.2004.827925.

Windhoff, M., Opitz, A., Thielscher, A., 2013. Electric field calculations in brain stimulation based on finite elements: an optimized processing pipeline for the generation and usage of accurate individual head models. Hum. Brain Mapp. 34 (4), 923–935. https://doi.org/10.1002/hbm.21479.

Yachou, Y., Bouaziz, N., Makdah, G., Senova, Y.S., Januel, D., Pelissolo, A., et al., 2025. Transcranial direct current stimulation in patients with depression: an electric field modeling meta-analysis. J. Affect. Disord. 374, 540–552. https://doi.org/10.1016/j.jad.2025.01.001.